Chemical Engineering and Processing 89 (2015) 41–53

Contents lists available at ScienceDirect

Chemical Engineering and Processing: Process Intensification

journal homepage: www.elsevier.com/locate/cep

Pharmaceutical crystallisation processes from batch to continuous operation using MSMPR stages: Modelling, design, and control

Qinglin Su [a], Zoltan K. Nagy [a,b], Chris D. Rielly [a,*]

[a] Department of Chemical Engineering, Loughborough University, Loughborough LE11 3TU, UK
[b] School of Chemical Engineering, Purdue University, West Lafayette, IN 47907-2100, USA

ARTICLE INFO

Article history:
Received 17 April 2014
Received in revised form 15 December 2014
Accepted 7 January 2015
Available online 8 January 2015

Keywords:
Antisolvent
Continuous crystallisation
MSMPR
Process design
C-control

ABSTRACT

In pharmaceuticals manufacturing, the conversion of conventional batch crystallisations to continuous mode has the potential for intensified, compact operation and more consistent production via quality-by-design. A pragmatic conversion approach is to utilise existing stirred tank batch crystallisers as continuous mixed-suspension mixed-product removal (MSMPR) stages. In this study, a rigorous and general mathematical model is developed for a pharmaceutical crystallisation process under continuous MSMPR operation. In the proposed changeover from batch to continuous operation, concentration control (C-control), which has been well accepted in batch crystallisation operation, is further extended to facilitate the convenient design of the steady-state operating point of a continuous MSMPR crystalliser; an objective is to ensure that the start-up procedures and on-line control conditions fall within the design-space of the original batch operation. Both single-stage and cascaded two-stage MSMPR crystallisers were investigated and compared to the conventional batch operation. It was observed that despite the production of a smaller number-based mean crystal size, the proposed continuous MSMPR operation achieved higher production capacity with shorter mean residence time and comparable product yield to the batch operation. Lastly, the robustness of C-control strategy against uncertainties in crystallisation kinetics was also demonstrated for the proposed continuous MSMPR operation.

1. Introduction

Crystallisation is an important unit operation for separation and purification in the process industries, such as in the pharmaceuticals, food, and fine chemicals sectors, in which a solid crystalline product with desired purity, size, and shape may be obtained from an impure feed solution. Conventionally, crystallisation processes are operated in batch mode to allow flexibility to respond to varying customised design requirements and changing market demands; however, this approach can also lead to increased manufacturing costs and batch-to-batch variations in product quality. The advent of patent expiration of many bulk drugs [1] has generated an increasing need to become more competitive through advanced manufacturing technologies [2]. Hence the development of continuous manufacturing and crystallisation techniques has received increasing interest and research effort from academic and industrial sectors in the past decade, due to the potential advantages of reduced costs, shorter development time, more robust scale-up and improved control performance [1,3,4].

To date, there are three main types of continuous crystalliser that have been widely investigated for this purpose, viz., the mixed-suspension mixed-product removal (MSMPR) reactor [5], the plug flow reactor (PFR) [6], and the continuous oscillatory baffled crystalliser (COBC) [7]. Currently, the most dominant crystalliser type used in the pharmaceutical industries for batch operations is based on a stirred tank design. In addition, quantitative quality risk assessments of new continuous crystalliser platforms are not yet fully understood and there is limited information regarding their implementation on commercial scale plant installations [1]. The approval of new process platforms will be strictly regulated and therefore it may be practical to gradually convert existing batch operations to continuous mode by operating the stirred tank in an MSMPR mode. Such a changeover could be easier and more cost-effective than replacing existing capital equipment with completely new continuous crystalliser designs [8].

Towards this end, recent experimental and engineering efforts have been devoted to the implementation of continuous MSMPR crystallisers for pharmaceutical and fine chemical compounds. For

* Corresponding author. Tel.: +44 1509 222504.
E-mail address: C.D.Rielly@lboro.ac.uk (C.D. Rielly).

http://dx.doi.org/10.1016/j.cep.2015.01.001
0255-2701/

example, Sen et al. [9] optimised the start-up of a continuous pharmaceutical manufacturing process, wherein the cooling schedule of a continuous MSMPR crystalliser was taken into account. Griffin et al. [10] studied the integration and application of product classification and a recycle stream to a continuous MSMPR crystalliser, in order to obtain a small mean crystal size with a narrow size distribution. Similar studies of a continuous MSMPR crystalliser with a recycle stream for cooling and combined cooling–antisolvent crystallisations were reported by Wong et al. [11]. Furthermore, a series of investigations on cascaded multi-stage, continuous MSMPR crystallisers were conducted for cooling, antisolvent, and reactive crystallisations at the Novartis-MIT Center [12–14].

For many years, researchers and designers have made modelling assumptions and applied equations for MSMPR crystallisers, which were originally developed for sparingly soluble inorganic solute systems, by considering negligible solute and solid volumes [5], and have applied them to more highly soluble pharmaceutical compounds. This can lead to inaccurate calculation of the solute concentration, slurry volume, and mean residence time in a continuous operation. In some models the solute concentration and crystal size distribution are expressed per unit mass of solvent, but the nucleation kinetics are most often written per volume of solution; hence unit conversions of the kinetic equations are often necessary to incorporate them into the mass balance and population balance equations, during which the solute and solid volumes are often neglected [15]. Therefore, an aim of the current work is to develop a general mathematical modelling framework for an MSMPR crystalliser intended for pharmaceutical and fine chemical industries, by more rigorously taking into account solute and solid volumes, upon which the changing operations from batch to continuous crystallisation mode by MSMPR could be studied, optimised, and controlled.

The concentration control (C-control) approach is well known for its robustness against uncertainties in crystallisation kinetics, since it was originally designed for batch crystallisation control. The general idea of C-control is to determine an optimal solute concentration or supersaturation trajectory in the phase diagram, for example, concentration vs. temperature or concentration vs. antisolvent mass fraction; a feedback control system is then designed to maintain the optimal relationship between these state variables [16–19]. Detailed uncertainty and disturbance analyses carried out both experimentally and in simulations have shown that the approach ensures the consistent production of large crystals by suppressing excessive nucleation and the formation of undesired polymorphs [17,18,20–22]. In light of this, it would be useful to extend and exploit the robustness of C-control, with minimal additional effort, for the changeover from batch to continuous operations. One of the possible ways is to start up the crystallisation process following the optimal solute concentration trajectory [23–25], as in batch operation, and then switch to continuous operation after the solute concentration reaches a certain point on the optimal concentration trajectory. Control loops are then implemented to regulate the crystalliser temperature and the addition of fresh solution and/or antisolvent in order to maintain the continuous operation at this specific point. In such a way, all the conversion procedures, from batch to continuous operation, are within the design-space of the original batch process, which should have been approved already by regulatory agencies.

To sum up accordingly, the present study considers a rigorous and general modelling framework for a crystallisation process using a stirred tank design which is seldom discussed in the open literature. Additionally, to the authors' knowledge, this is the first time that a pragmatic solution is investigated for converting existing batch crystallisation operation and its control technique to continuous mode.

This paper is organised as follows. The following section briefly describes the development of a rigorous and general modelling framework for crystallisation process. In Section 3, the idea of designing and controlling continuous MSMPR crystallisers is discussed based on the optimal solute concentration trajectory in C-control. Section 4 considers the application of the proposed modelling framework to a batch antisolvent crystallisation process and compares the result to that obtained using conventional modelling assumptions or Process Systems Enterprise (PSE)'s gCRYSTAL package. The changeover and control from batch to continuous operation using single-stage and cascaded two-stage MSMPR crystallisers are also demonstrated and discussed. Finally, concluding remarks are made in Section 5.

2. Rigorous modelling of a continuous MSMPR crystalliser

Crystallisation has a long history in the process industries for separation and purification operations. Mathematical modelling of continuous MSMPR crystallisers can be dated back to the 1950s or even earlier [26]. A conventional assumption is that the dissolution and crystallisation of solid crystals results in negligible volume changes to the solution; or equivalently those volumes of solute and solid crystals in the solution are assumed to be negligible. Such assumptions have been widely applied for sparingly soluble inorganic solutes, which form the "thin-suspension" solutions [5]. For example, for a population balance over a macroscopic region V with perfect mixing, defined as the solids-free volume, m^3, as shown below,

$$V\left(\frac{\partial n}{\partial t}+G\frac{\partial n}{\partial L}\right)+n\frac{dV}{dt}=-\sum_k L_k n_k \tag{1}$$

$$\frac{dV}{dt}=\int_{S_s} v\,dS-\int_{S_e} v\,dS=\frac{dV_s}{dt}-\frac{dV_e}{dt} \tag{2}$$

where n is the population density based on solids-free volume, $\#\,m^{-3}$; G is the crystal growth rate, $m\,s^{-1}$; L is the characteristic length of crystal, m; L_k is the input and output flow rate of solids-free liquid with a population density n_k, $m^3\,s^{-1}$; S_s is the free surface of the solids-free liquid, m^2; S_e is the total particle-fluid interface, m^2; v is the average velocity normal to the surface, $m\,s^{-1}$; V_s is the change at the free surface of the solids-free volume of liquid and V_e is the volume occupied by the solids, m^3. It is in Eq. (2) where the conventional assumptions are applied, viz., only the solvent or antisolvent additions are considered for V_s, while the V_e term is completely neglected for the case of the "thin suspension" solution.

It is noted that recent studies of pharmaceutical crystallisations, either batch or continuous, usually employed the population balance and mass balance equations based on these assumptions. However, this kind of assumptions may be a problem for highly soluble solute systems in pharmaceutical and fine chemical crystallisation processes and, in particular, when the product yield is high. For example, the solubility of paracetamol in isopropanol and water mixtures could be high around 200 g per kg of solvents and with a reported molar volume of 128.82 $cm^3\,mol^{-1}$ or 1174 $kg\,m^{-3}$ for the mass density [27]. On the other hand, the density of solid paracetamol crystal is reported as 1263 $kg\,m^{-3}$. Therefore, neglecting paracetamol solute and crystal volumes, or their volume changes, can lead to incorrect calculation of solute concentration, nucleation rate, and some volumetric properties, such as the solution volume. Furthermore, the solution volume, slurry density, and mean residence time are more important variables for continuous crystalliser design than for batch operations.

Hence, rigorous considerations of thermodynamic properties, such as the partial molar volumes of solute and solvents, molar

volume of crystal, are important and necessary for a continuous MSMPR crystalliser designed for use in the pharmaceutical and fine chemical industries. In this study, a general and rigorous modelling framework is developed for a stirred tank crystalliser, which can be used for cooling and antisolvent crystallisations in either batch/semi-batch or continuous modes.

The proposed modelling framework is also derived from the population balance of Eq. (1), while the population density, $f(L)$, is based on the total volume of the system slurry (V_{slurry}) instead, as illustrated below. Thus the explicit calculation of Eq. (2) could be avoided.

$$\frac{\partial f}{\partial t} + G\frac{\partial f}{\partial L} = -\sum_k Q_k n_k \tag{3}$$

$$f = nV_{slurry} = n(V_{liquid} + V_{solid}) \tag{4}$$

where f is the population density based on total slurry volume, #; Q_k is the slurry volumetric flow rate of stream k to/from crystalliser, $m^3\,s^{-1}$; V_{liquid} and V_{solid} are the liquid and solid volume in crystalliser, respectively, m^3.

The standard method of moments is then applied to Eq. (3) which leads to the moments of the crystal size distribution in the total slurry volume. The proposed modelling framework is demonstrated as follows, where mass balances for components, such as solute, solvent, antisolvent, and crystal, are also included. Incidentally, it is assumed that the nucleation occurs only in the liquid solution as indicated in Eqs. (5) and (9)–(12).

$$\frac{dN_{solute}}{dt} = \sum_k F_k x_{k,solute} - \frac{K_v}{v_{cry}}(3GM_2 + V_{liquid}Br_0^3) \tag{5}$$

$$\frac{dN_{solvent}}{dt} = \sum_k F_k x_{k,solvent} \tag{6}$$

$$\frac{dN_{anti}}{dt} = \sum_k F_k x_{k,anti} \tag{7}$$

$$\frac{dN_{cry}}{dt} = \sum_k F_k x_{k,cry} + \frac{K_v}{v_{cry}}(3GM_2 + V_{liquid}Br_0^3) \tag{8}$$

$$\frac{dM_0}{dt} = \sum_k Q_k \mu_{0,k} + V_{liquid}Br_0^0 \tag{9}$$

$$\frac{dM_1}{dt} = \sum_k Q_k \mu_{1,k} + V_{liquid}Br_0^1 + GM_0 \tag{10}$$

$$\frac{dM_2}{dt} = \sum_k Q_k \mu_{2,k} + V_{liquid}Br_0^2 + 2GM_1 \tag{11}$$

$$\frac{dM_3}{dt} = \sum_k Q_k \mu_{3,k} + V_{liquid}Br_0^3 + 3GM_2 \tag{12}$$

$$M_j = \int L^j f(L)dLj = 0, 1, 2, 3 \tag{13}$$

$$V_{liquid} = \sum_{i=1}^{3} N_i \bar{v}_i, i \neq cry \tag{14}$$

$$V_{solid} = N_{cry} v_{cry} \tag{15}$$

where N_i is the total moles of component i in the crystalliser, mol; F_k is the slurry molar flow rate of stream k to/from crystalliser, $mol\,s^{-1}$; $x_{k,i}$ is the mole fraction of component i in stream k; K_v is the volume shape factor of crystal; v_{cry} is the molar volume of crystals, $m^3\,mol^{-1}$; $\bar{v}_i$ is the partial molar volume of component i in liquid solution, $m^3\,mol^{-1}$; G is the crystal growth rate, $m\,s^{-1}$; M_j is the jth moment of crystal size distribution in the crystalliser, m^j; B is the nucleation rate, $\#\,m^{-3}\,s^{-1}$; r_0 is the size of nuclei, m; $\mu_{j,k}$ is the jth moment per volume of slurry stream k, $m^j\,m^{-3}$. Note that volumes of liquid and solid are rigorously calculated from (partial) molar volumes in Eqs. (14) and (15).

3. From batch to continuous crystallisation using an MSMPR

Despite several advantages related to continuous processing, such as, high throughput, more straightforward scale-up, elimination of intermediate storage, and consistent production, the pharmaceutical industry has been slow to adopt the principle of continuous operation due to the high investment cost for new manufacturing equipment [28]. On the other hand, the strict regulation in pharmaceutical approval systems, e.g. FDA in US, EMA in Europe, could create regulatory uncertainty about the approval of the product when innovative and drastic changes are imposed on the current manufacturing process [9,29]. Nevertheless, changing the operation within the design-space of an approved process is well accepted and a regulatory post-approval of the process is not required [30], which has already opened up the possibility for process optimisation [31]. Toward this end, based on the existing stirred tank crystallisers, a conservative and practical transition from batch to continuous crystallisation is proposed, which constrains the changeover within the design-space of the original batch crystallisation process.

The concentration control (C-control) strategy was originally designed to control batch crystallisation processes by following a predefined optimal solute concentration vs. temperature or antisolvent mass fraction trajectory, which defines the design-space of the batch process. The C-control strategy is schematically shown in Fig. 1 for a batch crystallisation process [20]. This optimal trajectory is usually intended as a trade-off between nucleation and crystal growth, i.e. to restrict the supersaturation level to control nucleation rate, while maintaining a certain level of supersaturation to boost crystal growth. Such an approach generates a trajectory bounded between the metastable limit and solubility curve on the phase diagram, as indicated by line AB in Fig. 1. Fundamental cascaded PI control loops would usually suffice to track this optimal trajectory, due to the requirement for a monotonically decreasing solute concentration and relatively slow crystallisation kinetics under conservative supersaturation level; the robustness of the approach against uncertainties in crystallisation kinetics has been clearly explained and also demonstrated experimentally and in simulation [17–19].

The batch crystallisation operation requires repeated following of the predefined trajectory AB, which demands a great deal of control intervention to the system, such as regulating the cooling rate, varying the addition flow rate of antisolvent, charging and discharging the crystalliser. Without control, the batch operation trajectory is difficult to follow and hence the system is liable to suffer from inconsistent production with quality attributives varying from batch to batch. Although C-control is robust, there is an associated cost due to its conservativeness in the supersaturation level. In fact, relatively long batch time may often be required to compensate for the uncertainties in crystallisation kinetics [17–19]. On the contrary, a continuous crystallisation

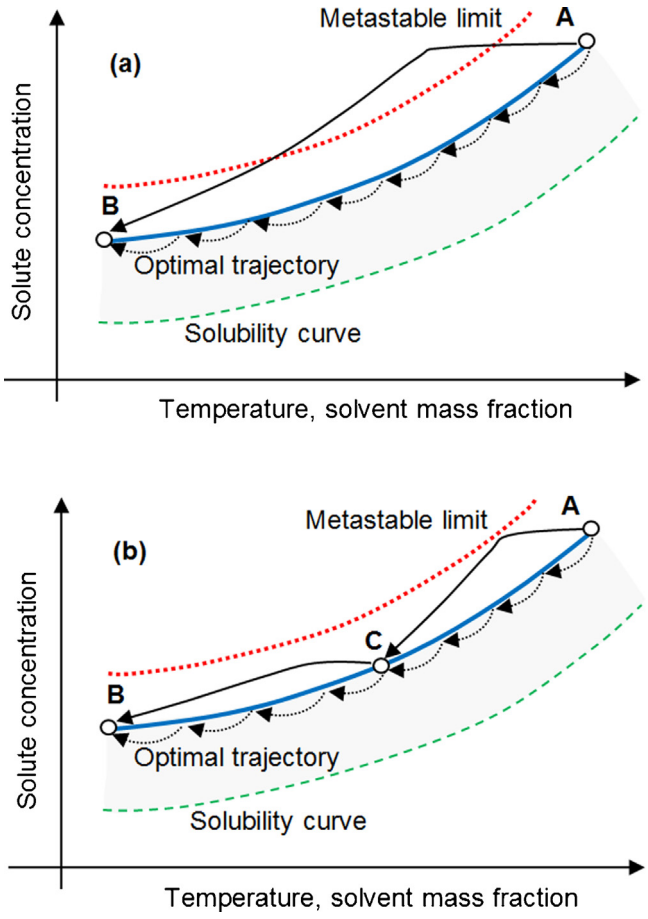

Fig. 1. Schematic of the C-control strategy for batch crystallisation process and its applications to start-up of continuous crystallisation process: (a) single-stage (b) two-stage (continuous arrow line: general start-up; dash arrow line: C-control start-up).

process would maintain its operation at a steady-state operating point (or a set of operating points for distributed systems), demanding fewer regulating control efforts and assuring more consistent production of crystals. The steady-state operating point (s) of a continuous process would naturally be located on the optimal trajectory shown in Fig. 1, so long as this trajectory makes the best trade-off between nucleation and crystal growth. With an aim of quick development and making minimum changes to the whole manufacturing streamline, the changeover from batch to continuous mode of a current crystallisation process would be conservative by setting the steady-state operating point to be at the end of this optimal trajectory, viz., point B in Fig. 1(a) for a single-stage MSMPR crystallisation process; thus the same product yield and similar quality attributives could be expected.

On the other hand, it is also obvious from Fig. 1(a) that one possible way of starting up a continuous crystallisation process from point A, to reach the MSMPR operation at point B, is to first operate the stirred-tank crystalliser as a normal batch operation following the optimal trajectory AB by C-control strategy and then to shift to continuous MSMPR operation by streaming solution in and out of the crystalliser while maintaining constant slurry volume when the system reaches at point B, as shown by the dash arrow line in Fig. 1(a). Thus, the production of off-spec material during the initial transient start-up of a continuous process could be minimised. Beside the PI control loop for C-control implementation during start-up, PI control loops could also be added under the same idea of C-control to maintain the steady-state operation at point B by manipulating the flow rate of coolant to the jacket, or feeding fresh solution and antisolvent to the crystalliser. The cooling down of the feed solution A, or directly mixing it with large amount of antisolvent, in the start-up of a continuous MSMPR crystalliser to reach the operating point B, (known as the general start-up procedure), could possibly generate relatively high supersaturation and hence induce uncontrolled nucleation as illustrated in Fig. 1(a) by the continuous arrow line. In contrast, the proposed start-up operation for continuous MSMPR crystallisation by C-control is able to ensure that the start-up procedures and operating point(s) are well-controlled and well maintained within the design-space of the original batch crystallisation process.

Note that it is very common for pharmaceutical industries to employ parallel production lines for batch operation to increase processing capacity. Hence, cascaded multi-stage continuous MSMPR crystallisers would be an interesting alternative for transferring current parallel batch operation to cascaded continuous mode by connecting several stirred tank crystallisers in sequence. Analogously, for multi-stage continuous process, the operating point for the last stage could also be set at point B, and identical start-up procedures and online control could be applied as well, as shown in Fig. 1(b). Without any loss of generality, the following section discusses the design of a cascaded two-stage arrangement. The extension to cascaded arrangements with more than two stages is straightforward.

The steady-state operating point of the first stage crystalliser is located in between the starting point A and the end point B of the optimal trajectory, viz., point C in Fig. 1(b). Likewise, the first stage crystalliser could be started up to reach the operating point C by following the optimal trajectory from A to C using the C-control strategy and then maintained at its steady-state operating point at C. Suppose the total batch time from A to B is t_B, and the time needed for the batch process going from A to C is t_C, then the start-up procedure of this two-stage crystallisation process could be scheduled, such that the last stage crystalliser starts earlier as a normal batch crystalliser from A to B, then followed by the start of the first stage crystalliser at time t_B–t_C (also as a batch moving to point C from A) so that they can reach their steady-state operating points of B and C, respectively, at the same time, viz., at time t_B. Then the changeover from batch to continuous operation for the cascaded arrangement can be completed seamlessly. This start-up method is also within the design-space of the batch crystallisation process and avoids the risk of introducing large nucleation rates when compared to the general start-up procedure that initialises the cascaded crystallisers in sequence, as shown in Fig. 1(b); in that case the two stages also reach their steady-state operations in sequence.

Furthermore, for the design of a general n-stage cascaded crystallisers as shown in Fig. 2, the optimal selection of the operating points for the first $(n-1)$ stages could be considered, in which the following objective function is minimised:

$$\underset{C_{i,\mathrm{set}},T_{i,\mathrm{set}},M_{i,\mathrm{set}},\gamma_i}{\mathrm{MIN}} J_{ss}(\mathbf{P}_n) + \sum_{j}^{n} \mathbf{E}_j \mathbf{W} \mathbf{E}_j^T \tag{16}$$

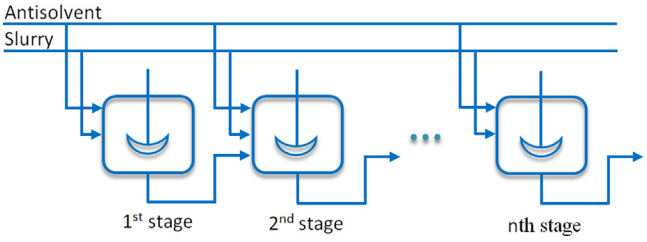

Fig. 2. Schematic of general n-stage cascaded crystallisers.

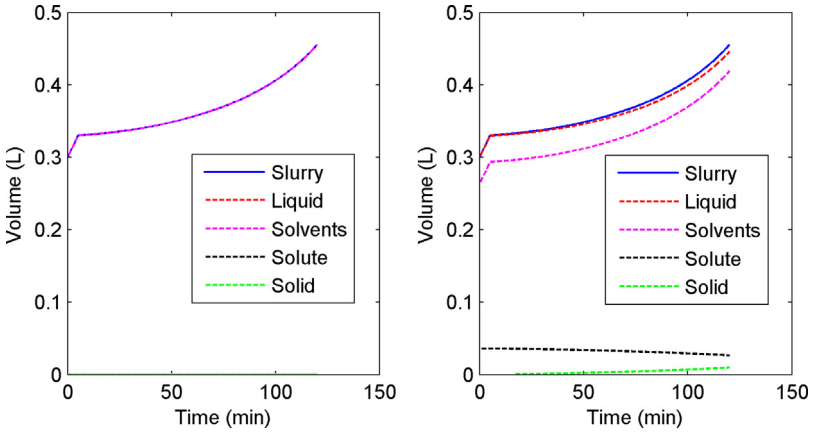

Fig. 3. Comparison of slurry volume between case (1) negligible solute & solid volume (left) and case (2) rigorous modelling under ideal mixing (right). (Legend arranged in descending order of volume, same as Fig. 8).

subject to

$$i = 1, 2, \ldots, n-1 \tag{17}$$

$$j = 1, 2, \ldots, n \tag{18}$$

$$\mathbf{E}_j = \left[C_{j,\mathrm{ss}} - C_{j,\mathrm{set}}, T_{j,\mathrm{ss}} - T_{j,\mathrm{set}}, M_{j,\mathrm{ss}} - M_{j,\mathrm{set}}\right] \tag{19}$$

$$f(C_{i,\mathrm{set}}, T_{i,\mathrm{set}}, M_{i,\mathrm{set}}, V_{i,\mathrm{batch}}) = 0 \tag{20}$$

$$\gamma_i V_{i,\mathrm{batch}} \leq V_{\max} \tag{21}$$

$$C_{j,\mathrm{set}} \leq C_{j-1,\mathrm{set}} \tag{22}$$

where J_{ss} is the objective function at steady state operation; $\mathbf{P}_n$ is the product qualities at the exit of the nth stage crystalliser; $\mathbf{E}_j$ is the control error for the jth stage crystalliser at steady state; $\mathbf{W}$ is a diagonal weighting matrix; $C_{j,\mathrm{ss}}$ is the solute concentration of jth stage crystalliser at steady state; $C_{j,\mathrm{set}}$ is the set point for concentration of the jth stage crystalliser; similar definitions apply to temperature (T) and antisolvent mass fraction (M); $V_{i,\mathrm{batch}}$ is the corresponding volume when a normal batch crystalliser follows the optimal trajectory and reaches the ith stage operating point ($C_{i,\mathrm{set}}$,$T_{i,\mathrm{set}}$, $M_{i,\mathrm{set}}$) under a nominal batch operation f; γ_i is the scaling up factor for the ith stage crystalliser; hence, $\gamma_i V_{i,\mathrm{batch}}$ is the actual operating volume of ith stage crystalliser at steady state; $V_{\max}$ is the maximum allowable operating volume for a stirred tank crystalliser. It is worth pointing out that for a semi-batch antisolvent crystallisation, $V_{i,\mathrm{batch}}$

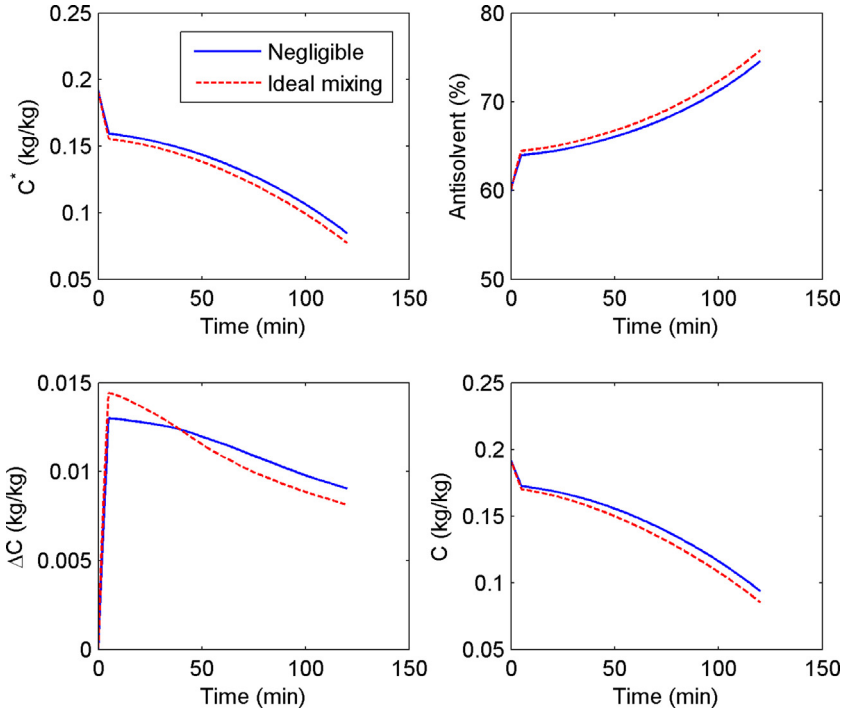

Fig. 4. Comparison of concentrations between case (1) negligible solute & solid volume and case (2) rigorous modelling under ideal mixing assumption.

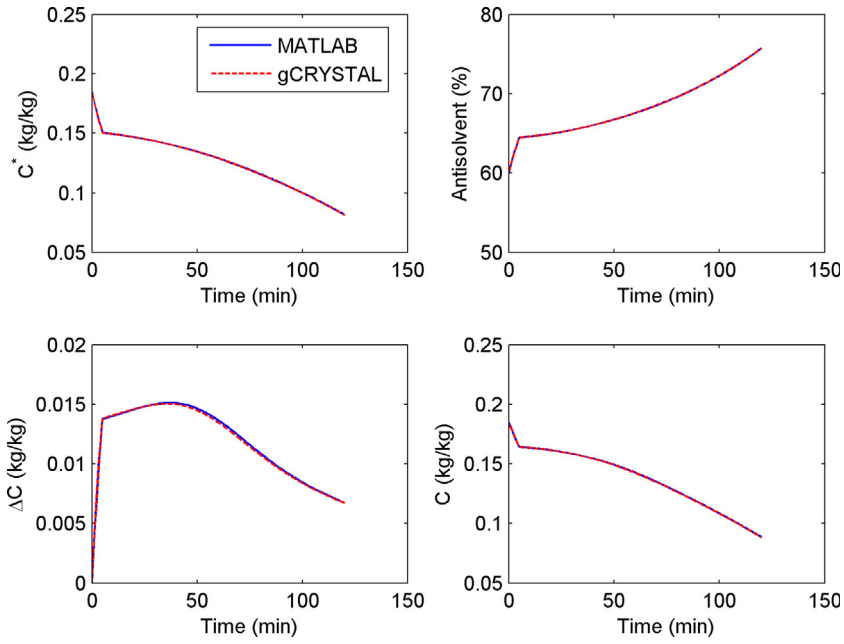

Fig. 5. Comparison of concentrations between rigorous modelling in MATLAB and in gCRYSTAL.

increases with a decrease of $C_{j,\mathrm{set}}$ in a nominal batch operation f due to the continuous addition of antisolvent. For example, if $C_{j,\mathrm{set}}$ is chosen close to the starting point A as in Fig. 1(b), then the operating volume of jth crystalliser $V_{i,\mathrm{batch}}$ would be far smaller than the maximum allowable operating volume $V_{\max}$. Thus an additional scaling up factor γ_i is introduced to optimise the respective operating volumes of the first $(n-1)$ crystallisers at steady state. The constraint (22) is to confirm that the operating points of concentration are in a descending order along the stages. It is also noted that a large penalty weight of $\mathbf{W}$ on the control error in the objective function (16) would make sure all the steady-state operating points are attainable for the cascaded multi-stage crystallisers. Incidentally, once the operating points are chosen, the distributions of fresh slurry or antisolvent are regulated by the PI control loops in order to maintain their respective steady-state operating points.

4. Results and discussion

4.1. Rigorous modelling and verification

To demonstrate the potential use of a rigorous modelling approach in pharmaceutical crystallisation, the developed model is applied, based on the MATLAB R2013b platform, for a semi-batch

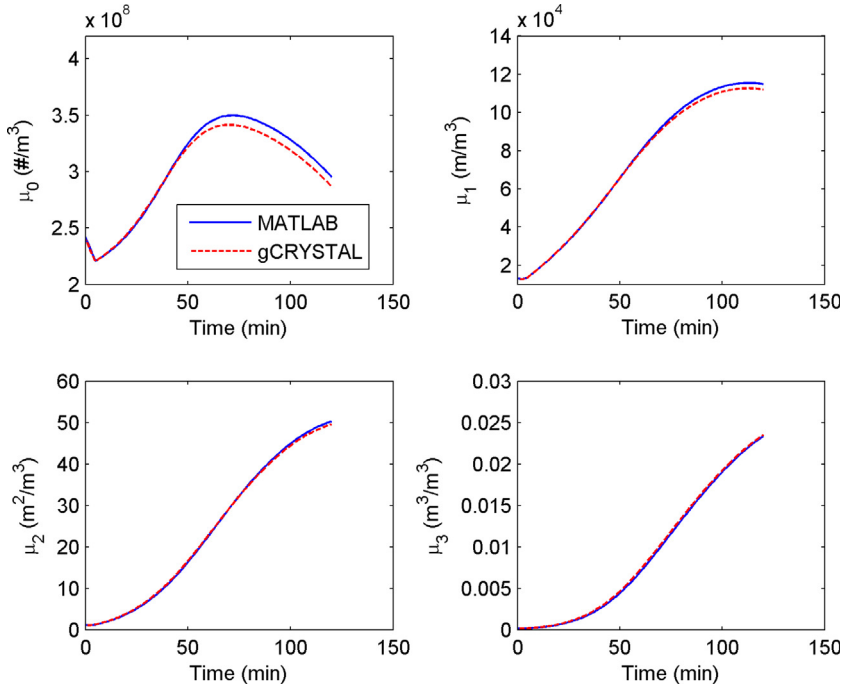

Fig. 6. Comparison of moments of crystal size distribution between rigorous modelling in MATLAB and in gCRYSTAL.

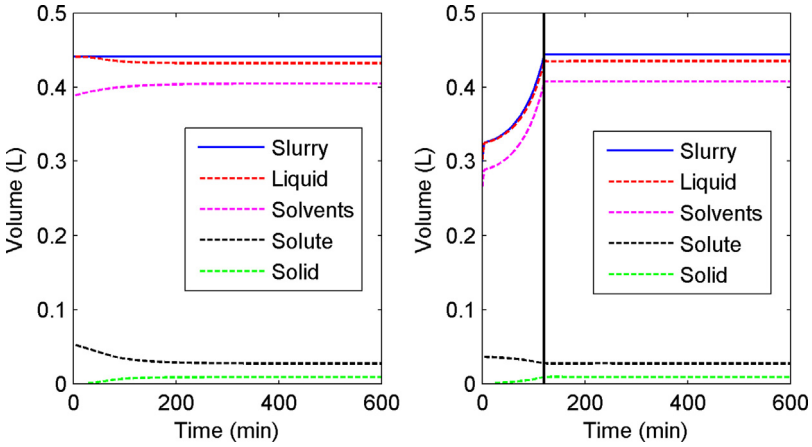

Fig. 7. Comparison of slurry volume between general start-up (left) and proposed start-up (right) (the vertical line at 120 min shows the changeover from batch to continuous crystallization for the proposed start-up, same as Figs. 8–10).

antisolvent crystallisation using paracetamol in acetone and water (antisolvent) mixture in a stirred tank crystalliser [20]. The crystalliser is first initialised with 0.30 L of a seeded solution (seed mass = 0.4125 g, number-mean size 187.50 μm) saturated at an antisolvent mass fraction of 0.60. Continuous addition of antisolvent is then introduced to increase the supersaturation during a batch time of 2 h. For more details of the experiment, crystallisation kinetics and solubility, readers are referred to the original reference in [20]. The resulting antisolvent addition flow rate profile is determined by the C-control strategy to constantly trade off the nucleation and crystal growth and is considered for two cases where different assumptions are applied for the calculation of volumes of the components in the crystalliser. Case (1) assumes negligible (partial) molar volumes for solute and solid, except in Eqs. (5) and (8) for the sake of the solute mass balance, which should correspond to the results shown in [20]. In contrast, case (2) considered the ideal mixing rule,, constant molar volumes for all the components in the crystalliser.

Fig. 3 shows a comparison of the slurry volume and its components in the crystalliser for each of the two cases. The left plot shows case (1) in which the simulation assumes negligible solute and solid volume in solution, whereas the right one shows case (2) using the ideal mixing rule. It is observed in the right plot that the solute volume occupies a significant portion in the liquid and it decreases as the solute precipitates out as crystals. However, under the assumption of negligible solute and solid volume, the solvents volume is greater, which affects the solute solubility and concentration as indicated in Fig. 4. Significant differences in the absolute supersaturation are also observed, which have a great impact on the simulation of primary nucleation and the resulting amount of fine crystals. Therefore, it is interesting and necessary to apply a rigorous modelling framework to crystallisation systems that contain highly soluble solute in pharmaceutical and fine chemical industries.

It should be pointed out here that the model compound of paracetamol (acetaminophen) is still a small molecule with a molecular weight of 151 g mol^{-1} and thus constant (partial) molar volumes are assumed here. Furthermore, due to the low yield, the change of overall slurry volume due to the crystallisation effect is not so obvious. However, for therapeutic proteins that have complex molecular structure and varying partial molar volumes due to the change of solution pH value or ion strength, their

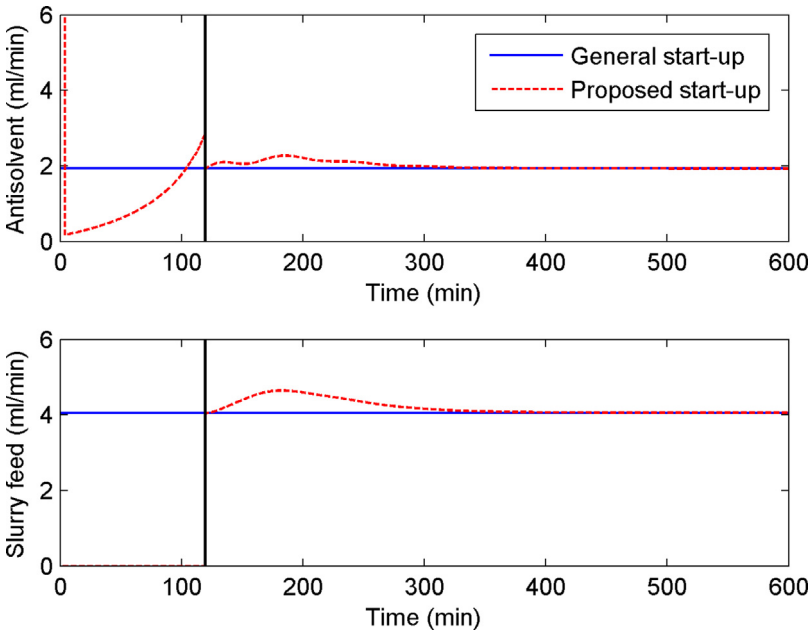

Fig. 8. Comparison of antisolvent and fresh slurry feeding between general start-up and proposed start-up.

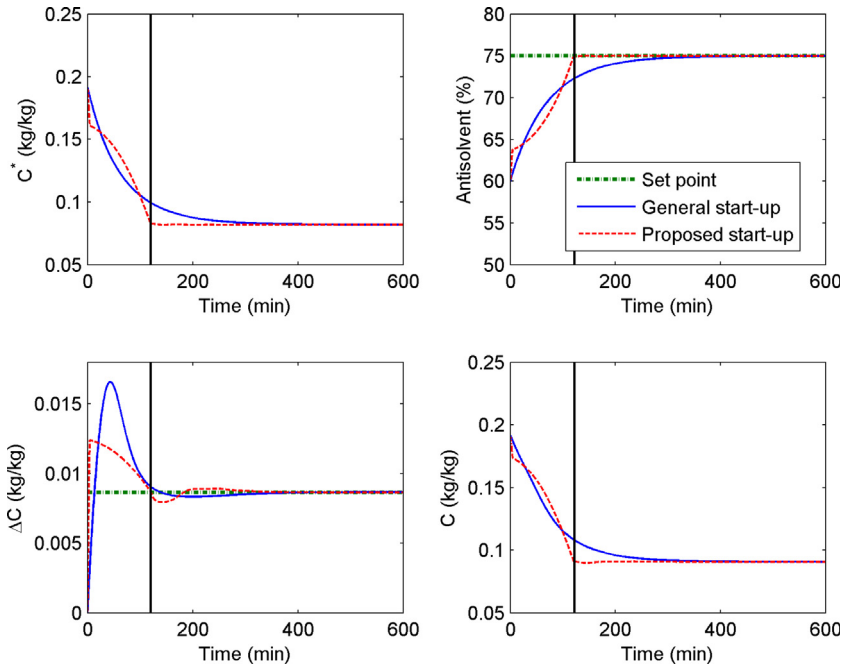

Fig. 9. Comparison of concentrations between general start-up and proposed start-up.

corresponding crystallisation effects could be much more significant and important, as suggested in [16].

To further verify the developed rigorous modelling framework, another simulation of the above antisolvent crystallisation process was performed in gCRYSTAL v3.0 but with a different seed loading (gCRYSTAL requires the seed crystal size distribution, while only moments are provided by Woo et al. [20] and hence a new seed loading with log-normal crystal size distribution (mean location = 180 μm, standard deviation = 2.0) was considered here while others remain the same). In addition, the calculated initial moments in gCRYSTAL were also input to the rigorous model considering the ideal mixing rule and simulated in MATLAB R2013b. The ideal mixing rule is implemented in gCRYSTAL and thus nearly identical results should be obtained for the two platforms, verifying the rigorous model development in the above section. Comparisons between the two sets of results are shown in Figs. 5 and 6. Excellent agreement in the predicted solute concentrations were obtained, while the small mismatches in the moments could be due to the different formulation and solution of the partial differential equation (PDE) for the population balance model. In gCRYSTAL, the population balance PDE is discretised using central finite difference approximations

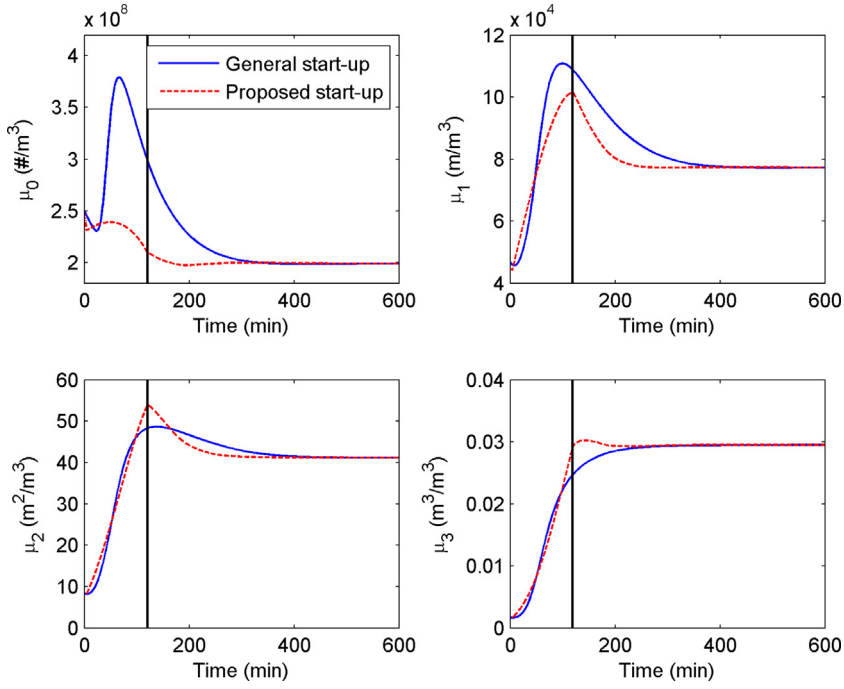

Fig. 10. Comparison of moments of crystal size distribution between general start-up and proposed start-up.

into a set of ordinary differential equations (ODEs), which are solved using the method of backward differential formula (BDF). In contrast, the rigorous model implemented here in MATLAB converts the population balance PDE into a set of moment-based ODEs, as shown in Eqs. (9)–(12), which are then solved numerically using ODE45 (Runge–Kutta).

4.2. Continuous crystallisation using MSMPR

To demonstrate the proposed idea of converting batch crystalliser into continuous one using MSMPR operation, the aforementioned paracetamol crystallisation process in [20] is further employed. The optimal concentration vs. antisolvent mass fraction trajectory for C-control strategy therein is also adopted here to facilitate the proposed process design of MSMPR crystalliser. Note that this optimal trajectory is solely based on a constant trade-off between the nucleation and crystal growth kinetics,

$$K = \frac{G}{B} = \left(\frac{k_g \Delta C^g}{k_b \Delta C^b}\right) = 7 \times 10^{-2} \left(\frac{\mathrm{ms}^{-1}}{\mathrm{m}^{-3}\mathrm{s}^{-1}}\right) \tag{23}$$

$$\Delta C = \left(\frac{K k_b}{k_g}\right)^{1/(g-b)} \tag{24}$$

where K is the trade-off ratio. Hence its optimality is held whether or not the solute and solid crystal volumes are considered in this work. Nevertheless, the following simulations are based on the rigorous model under the ideal mixing rule within MATLAB R2013b.

For a single stirred tank crystalliser, as discussed in Section 3, the proposed start-up and changeover from batch to continuous operation can be taken as a normal batch operation followed by maintenance of its steady-state operating point at the optimal concentration trajectory by C-control, as can be seen in Figs. 7–10. The proposed start-up procedure first initialises the stirred tank crystalliser with 0.30 L seeded solution saturated at 60% water mass fraction, followed by the C-control procedure to reach the end point of the optimal concentration trajectory at time 120 min, and which finally stabilises its operation at this end point (see horizontal line in Fig 9). Thereafter, two PI control loops are used to control the antisolvent mass fraction and absolute supersaturation by regulating antisolvent addition and fresh slurry feeding, respectively (see the flow rates after the vertical line in Fig. 8). Incidentally, the slurry level in the crystalliser was kept constant by regulating the outflow of product stream as shown in Fig. 7. This start up method is contrasted with the general start-up procedure which was initially filled with 0.44 L of the same starting solution and directly pumps in/out using the steady-state flow rates of the proposed start-up procedure so that they have the same mean residence time under continuous operation and reach the same final steady-state point (see Figs. 7–10).

Compared to the general start-up, the proposed scheme gives a shortened time to steady state and avoids the initial large supersaturation and primary nucleation rate (μ_0, zeroth moment), as shown in Figs. 8 and 10. Furthermore, there is no product outflow with low yield that needs to be recycled or reworked during the proposed start-up, as a batch operation is adopted here and thus there is no exiting flow in the early transient stages. More importantly, the proposed operation could be regarded as being within the design-space of the batch operation, which should have been previously approved.

For a cascaded MSMPR design, by following Fig. 1(b) and the optimal design of Eqs. (16)–(22), two-stage MSMPR crystallisers (S1 and S2) in cascade are also designed in this work. An objective function maximising the number-based mean crystal size L_n is considered in the objective function of Eq. (16), which finds the operating point in the optimal concentration trajectory for the first stage crystalliser at 0.14 kg solute per kg solvents and 0.67 for concentration and antisolvent mass fraction, respectively; and a total operating volume of 0.35 L with a scaling up factor γ of 0.98 at steady-state. As previously mentioned, the second stage crystalliser is maintained at its steady-state operation at the end of the optimal concentration trajectory. It is interesting to point out that the scaling up factor is slightly lower than 1; this should be due to the penalty term in the optimisation problem (16) to make sure the operating points are attainable under continuous operation.

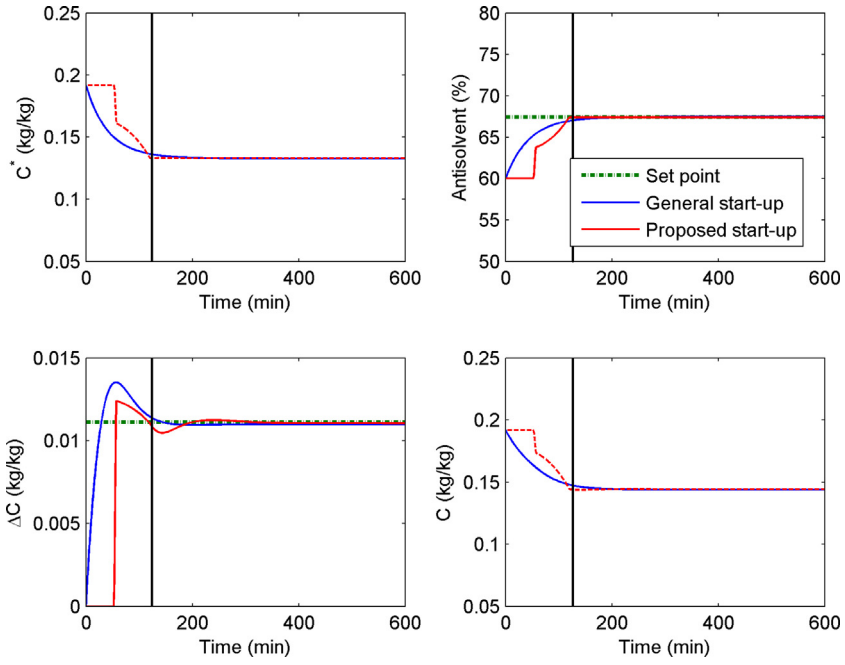

Fig. 11. Comparison of concentrations between general start-up and proposed start-up in the first stage crystalliser S1.

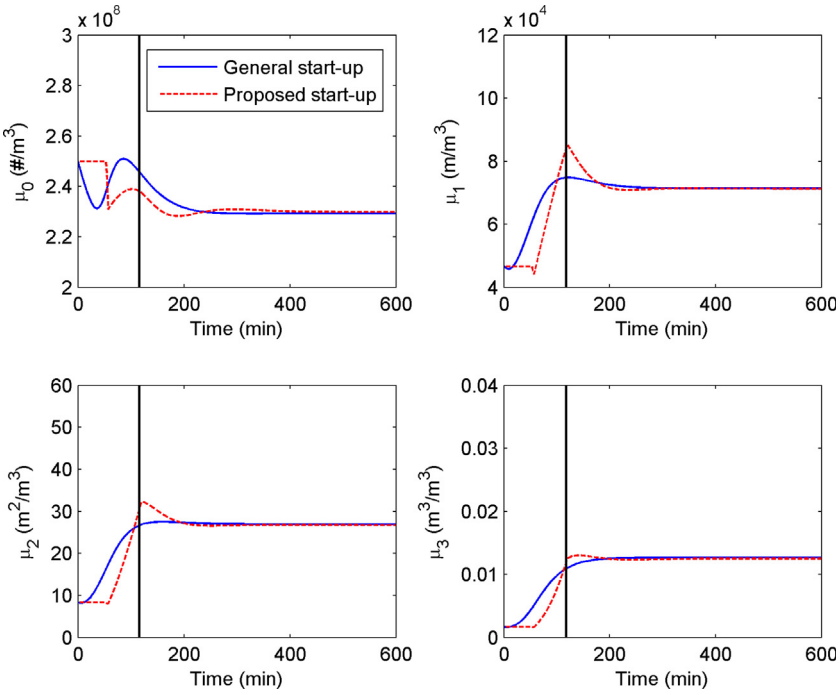

Fig. 12. Comparison of moments of crystal size distribution between general start-up and proposed start-up in the first stage crystalliser S1.

The proposed start-up operations of the two-stage crystallisers S1 and S2 can be seen in Figs. 11–13. While the crystalliser S2 is started as a normal batch process for the first 120 min, the crystalliser S1 is initially filled with (0.98×0.30) L starting seeded solution saturated at 0.60 antisolvent mass fraction and also held for 52.50 min, it then follows the optimal concentration trajectory by C-control to reach the set point, and finally settles down at this set point for continuous operation at the same time as the crystalliser S2 at 120 min (see the vertical line). Due to the low yield in crystalliser S1 (see Table 1), only marginal differences are observed between the general start-up and proposed start-up procedures in Figs. 11 and 12 in terms of time to steady state and primary nucleation rate. However, analogous to the case of a single MSMPR crystalliser, the second stage MSMPR crystalliser also shows a much faster approach to the designed operating points and avoids a large amount of primary nucleation during start-up operation (the results are similar to Figs. 9 and 10, but are not shown here). The distribution of antisolvent and slurry additions between the two-stage crystallisers

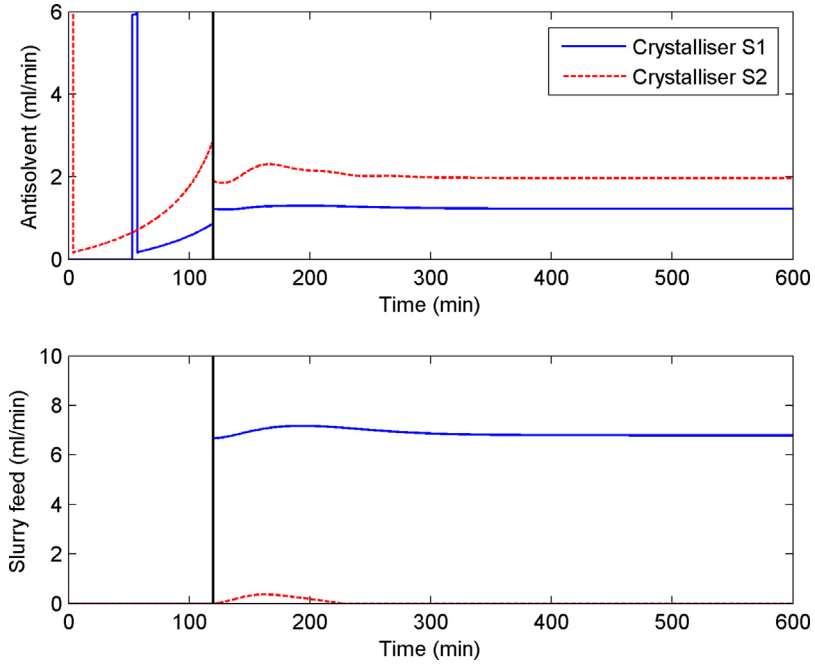

Fig. 13. Addition flow rates of antisolvent and fresh slurry for cascaded two-stage crystallisers.

Table 1
Comparison of different crystallization processes.

Processes	τ (min)	L_n (μm)	Yield (%)	Productivity ($g\,h^{-1}$)
Batch	120.00	484	26.40	6.03[a]
Continuous	73.81	389	24.34	9.03
Cascade S1	44.88	310	7.61	4.72
Cascade S2	45.03	422	23.97	14.88

[a] Down time for batch operation is not considered.

is shown in Fig 13. Interestingly, it is noted that all the slurry solution goes to the first stage crystalliser at the steady-state operation, which is consistent with the results found by Frawley [32] who also optimised a cascaded two-stage MSMPR crystalliser.

The overall steady-state performances are summarised and compared for the above batch crystalliser, continuous single-stage and cascaded two-stage MSMPR crystallisers in Table 1. There are smaller number mean crystal size and slightly lower yield for the continuous MSMPR operations; this is mainly due to the fact that primary nucleation rates are higher at higher antisolvent mass fraction where the continuous MSMPR operation points are located. Although, there are also relatively higher productivities of solid crystals, for shortened mean residence times of the feeding streams.

4.3. Online control of MSMPR crystallisers

The C-control strategy has been well acknowledged for its robustness against the uncertainties in crystallisation kinetics for batch crystallisation control (see Woo et al. [20] for full details of the C-control methodology). Hence it would be interesting to confirm the robustness of C-control in the current continuous MSMPR crystallisation process. Here we define "flow rate control"

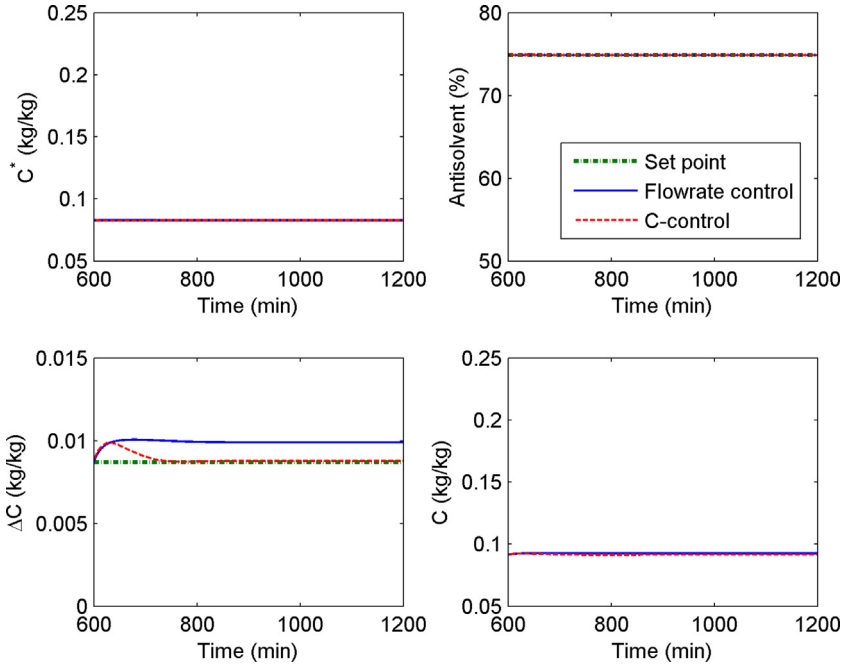

Fig. 14. Online control performances by flow rate control and C-control in crystalliser S2 under growth rate uncertainty.

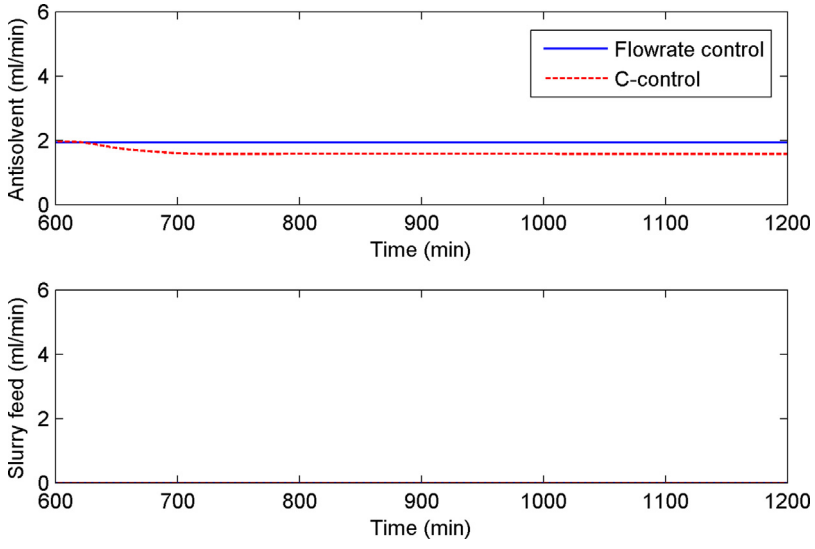

Fig. 15. Antisolvent flow rates to crystalliser S2 by flow rate control and C-control under growth rate uncertainty.

in which the addition flow rates of antisolvent and fresh seeded solution are controlled at their steady-state value, i.e. the same as the general start-up procedure. In contrast, the C-control approach maintains the antisolvent mass fraction and supersaturation at their respective steady-state set points by regulating the antisolvent addition and fresh slurry, respectively.

In Figs. 14 and 15, the crystal growth rate coefficient (k_g) is reduced by 20% from its nominal value and sluggish crystal growth occurs from 600 min onward. The performances of flow rate control and C-control for the 2nd stage crystalliser S2 in the cascaded two-stage MSMPR crystallisers are compared. By maintaining the steady-state antisolvent and fresh slurry flow rates (see Fig. 15); the flow rate control can hold the antisolvent mass fraction, and thus the solubility, at its steady-state value. However, the concentration and the supersaturation are disturbed from their steady-state values when the uncertainty in crystal growth rate occurs as shown in Fig. 14. On the contrary, the C-control procedure brings back the supersaturation at its steady-state set point while maintaining the antisolvent mass fraction by reducing the antisolvent feed rate (see Fig. 15). Interestingly, the fresh slurry feed rate is again kept constant at zero, the same as under normal steady-state operation. Both the antisolvent and fresh slurry feed rates were reduced in 1st stage crystalliser analogously (results not shown here) to account for the reduced crystal growth rate for paracetamol. Comparisons of the number-based mean crystal size for both control strategies are shown in Fig. 16, where the number mean crystal sizes are nearly retained at their previous steady-state values by C-control. Nevertheless, similar to the drawback of C-control in batch operation, which extends the batch time to tackle the sluggish crystal growth, the reduced addition flow rates by C-control for continuous operation also lead to lower productivity at steady state, i.e. from nominal 14.88 to 11.94 g h^{-1}, and longer mean residence time from nominal 89.91 to 105.27 min.

It is worth pointing out that, for moderate kinetic uncertainties in crystal growth rate (>80% reduction in k_g), the robustness of C-control over the flow rate control is also demonstrated; although a longer time to re-reach the steady state is required. However, for moderate kinetic uncertainties in nucleation rate coefficient (k_b), since the continuous MSMPR crystalliser is already operated at the optimal concentration vs. antisolvent mass fraction trajectory, that is assumed to be the best trade off the nucleation and crystal growth, they have no significant effects on the overall crystalliser performance, such as solute concentration, volume-based mean crystal size, etc. Hence the performance of flow rate control and C-control are comparable [20]. Additionally, similar performances were also observed when the C-control strategy was applied for online control of a single-stage continuous MSMPR crystalliser.

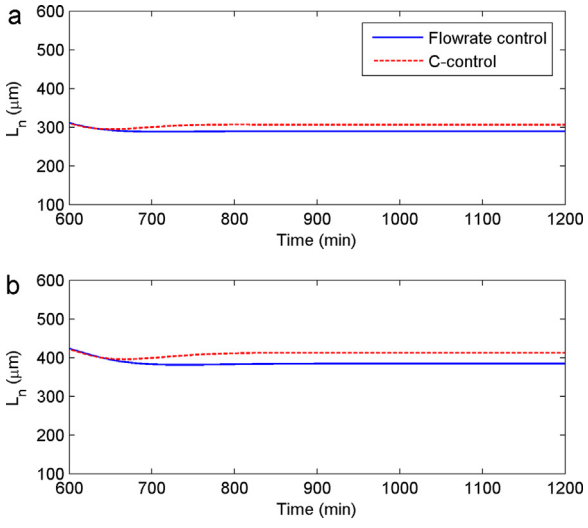

Fig. 16. Number-based mean crystal sizes in cascaded two-stage crystalliser under growth uncertainty (top: crystalliser S1; bottom: crystalliser S2).

5. Conclusions

The current study developed a general and rigorous mathematical modelling framework for continuous MSMPR crystallisers. The C-control strategy was further extended to facilitate the convenient design of a start-up procedure and online control technique for multi-stage continuous MSMPR crystallisers. Thereby, the changeover from existing batch stirred-tank operation to continuous MSMPR operation is well-within the design-space of the original batch operation. It is observed that despite the smaller mean crystal size, the proposed continuous MSMPR operation achieves higher production capacity with shorter mean residence time and comparable product yield as in batch. The robustness of C-control strategy against uncertainties in crystallisation kinetics was also demonstrated for the proposed continuous MSMPR operation.

Acknowledgements

The authors would like to acknowledge financial support from the UK EPSRC, AstraZeneca and GSK. The authors are also grateful for useful discussions with industrial partners from AstraZeneca, GSK, Mettler-Toledo, Perceptive Engineering and Process Systems Enterprise. This work was performed as part of the 'Intelligent Decision Support and Control Technologies for Continuous Manufacturing and Crystallisation of Pharmaceuticals and Fine Chemicals' (ICT-CMAC) Project (EP/K014250/1).

References

[1] B. Aksu, T. De Beer, S. Folestad, J. Ketolainen, H. Linden, J.A. Lopes, M. de Matas, W. Oostra, J. Rantanen, M. Weimer, Strategic funding priorities in the pharmaceutical sciences allied to quality by design (QbD) and process analytical technology (PAT), Eur. J. Pharm. Sci. 47 (2012) 402–405.
[2] K. Plumb, Continuous processing in the pharmaceutical industry changing the mindset, Chem. Eng. Res. Des. 83 (A6) (2005) 730–738.
[3] H. Leuenberger, New trends in the production of pharmaceutical granules: batch versus continuous processing, Eur. J. Pharm. Biopharm. 52 (2001) 289–296.
[4] S. Buchholz, Future manufacturing approaches in the chemical and pharmaceutical industry, Chem. Eng. Process. 49 (2010) 993–995.
[5] A.D. Randolph, M.A. Larson, Theory of Particulate Processes: Analysis and Techniques of Continuous Crystallization, Academic Press, San Diego, 1988.
[6] R.J.P. Eder, S. Radl, E. Schmitt, S. Innerhofer, M. Maier, H. Gruber-Woelfler, J.G. Khinast, Continuously seeded, continuously operated tubular crystallizer for the production of active pharmaceutical ingredients, Cryst. Growth Des. 10 (2010) 2247–2257.
[7] S. Lawton, G. Steele, P. Shering, L. Zhao, I. Laird, X.W. Ni, Continuous crystallization of pharmaceuticals using a continuous oscillatory baffled crystallizer, Org. Process Res. Dev. 13 (2009) 1357–1363.
[8] W.F. Banholzer, M.E. Jones, Chemical engineers must focus on practical solutions, AIChE J. 59 (2013) 2708–2720.
[9] M. Sen, A. Rogers, R. Singh, A. Chaudhury, J. John, M.G. Ierapetritou, R. Ramachandran, Flowsheet optimization of an integrated continuous purification-processing pharmaceutical manufacturing operation, Chem. Eng. Sci. 102 (2013) 56–66.
[10] D.W. Griffin, D.A. Mellichamp, M.F. Doherty, Reducing the mean size of API crystals by continuous manufacturing with product classification and recycle, Chem. Eng. Sci. 65 (2010) 5770–5780.
[11] S.Y. Wong, A.P. Tatusko, B.L. Trout, A.S. Myerson, Development of continuous crystallization processes using a single-stage mixed-suspension, mixed-product removal crystallizer with recycle, Cryst. Growth Des. 12 (2012) 5701–5707.
[12] A.J. Alvarez, A. Singh, A.S. Myerson, Crystallization of cyclosporine in a multistage continuous MSMPR crystallizer, Cryst. Growth Des. 11 (2011) 4392–4400.
[13] J.L. Quon, H. Zhang, A. Alvarez, J. Evans, A.S. Myerson, B.L. Trout, Continuous crystallization of Aliskiren Hemifumarate, Cryst. Growth Des. 12 (2012) 3036–3044.

[14] H. Zhang, J. Quon, A.J. Alvarez, J. Evans, A.S. Myerson, B. Trout, Development of continuous anti-solvent/cooling crystallization process using cascaded mixed suspension, mixed product removal crystallizers, Org. Process Res. Dev. 16 (2012) 915–924.
[15] P.J. Frawley, N.A. Mitchell, C.T. Ó'Ciardhá, K.W. Hutton, The effects of supersaturation, temperature, agitation and seed surface area on the secondary nucleation of paracetamol in ethanol solution, Chem. Eng. Sci. 75 (2012) 183–197.
[16] M. Fujiwara, Z.K. Nagy, J.W. Chew, R.D. Braatz, First-principles and direct design approaches for the control of pharmaceutical crystallization, J. Process Control 15 (2005) 493–504.
[17] G.X. Zhou, M. Fujiwara, X.Y. Woo, E. Rusli, H.H. Tung, C. Starbuck, O. Davidson, Z. Ge, R.D. Braatz, Direct design of pharmaceutical antisolvent crystallization through concentration control, Cryst. Growth Des. 6 (2006) 892–898.
[18] Z.K. Nagy, J.W. Chew, M. Fujiwara, R.D. Braatz, Comparative performance of concentration and temperature controlled batch crystallizations, J. Process Control 18 (2008) 399–407.
[19] Q.L. Su, R.D. Braatz, M.S. Chiu, JITL-based concentration control for semi-batch pH-shift reactive crystallization of L-glutamic acid, J. Process Control 24 (2013) 415–421.
[20] X.Y. Woo, Z.K. Nagy, R.B.H. Tan, R.D. Braatz, Adaptive concentration control of cooling and antisolvent crystallization with laser backscattering measurement, Cryst. Growth Des. 9 (2009) 182–191.
[21] C.S.N. Kee, B.H.R. Tan, R.D. Braatz, Selective crystallization of the metastable α-form of L-glutamic acid using concentration feedback control, Cryst. Growth Des. 9 (2009) 3044–3051.
[22] N.C.S. Kee, P.D. Arendt, R.B.H. Tan, R.D. Braatz, Selective crystallization of the metastable anhydrate form in the enantiotropic pseudo-dimorph system of L-phenylalanine using concentration feedback control, Cryst. Growth Des. 9 (2009) 3052–3061.
[23] B.G. Lipták, Controlling and optimizing chemical reactors, Chem. Eng. Mag. 93 (1986) 69–81.
[24] D. Bonvin, Optimal operation of batch reactors – a personal view, J. Process Control 8 (5) (1998) 355–368.
[25] D.E. Seborg, T.F. Edgar, D.A. Melliohamp, F.J. Doyle III, Process Dynamics and Control, third ed., John Wiley & Sons, New York, 2010.
[26] W.C. Saeman, Crystal-size distribution in mixed suspensions, AIChE J. 2 (1956) 107–112.
[27] H. Hojjati, S. Rohani, Measurement and prediction of solubility of paracetamol in water-isopropanol solution. Part 2. Prediction, Org. Process Res. Dev. 10 (2006) 1110–1118.
[28] J. Vercruysse, U. Delaet, I. Van Assche, P. Cappuyns, F. Arata, G. Caporicci, T. De Beer, J.P. Remon, C. Vervaet, Stability and repeatability of a continuous twin screw granulation and drying system, Eur. J. Pharm. Biopharm. 85 (2013) 1031–1038.
[29] Y. Gonnissen, S.I.V. Goncalves, B.G. De Geest, J.P. Remon, C. Vervaet, Process design applied to optimise a directly compressible powder produced via a continuous manufacturing process, Eur. J. Pharm. Biopharm. 68 (2008) 760–770.
[30] K.V. Gernaey, A.E. Cervera-Padrell, J.M. Woodley, A perspective on PSE in pharmaceutical process development and innovation, Comp. Chem. Eng. 42 (2012) 15–29.
[31] Z.K. Nagy, M. Fujiwara, R.D. Braatz, Modelling and control of combined cooling and antisolvent crystallization processes, J. Process Control 18 (2008) 856–864.
[32] P.J. Frawley, Process Crystallization: Kinetics to Optimization. Seminar presentation in Loughborough University, 2014.